International Journal of Fracture **82:** 253–266, 1996.

Strengthening of concrete prisms using the plate-bonding technique

Nonlinear fracture mechanics derivations applied to plates of steel or carbon fibre, bonded to concrete and loaded in shear

BJÖRN TÄLJSTEN
Division of Structural Engineering, Department of Civil Engineering, Luleå University of Technology, S-971 87 Luleå, Sweden

Received 25 October 1995; accepted in revised form 5 September 1996

Abstract. This paper presents the use of fracture mechanics for the plate bonding technique. Plates of steel or carbon-fibre reinforced plastic are bonded with an epoxy adhesive to rectangular concrete prisms and loaded in shear up to failure, what is normally known in fracture mechanics as mode II failure. In this special application a linear and a nonlinear approach are presented. The nonlinear equation derived for a realistic shear-deformation curve can only be used for numerical calculations. However, for simplified shear-deformation curves, the derived formula can be solved analytically. Results from tests, which are compared with the theory, are also presented.

Notation and symbols

A	= cross-section [m^2]
A_1	= cross-sectional area, adherent no. 1 [m^2]
A_2	= cross-sectional area, adherent no. 2 [m^2]
a	= crack length [m]
b	= width of strengthening plate [m]
C	= compliance [m/N]
E	= modulus of elasticity [Pa]
E_1	= modulus of elasticity, adherent no. 1 [Pa]
E_2	= modulus of elasticity, adherent no. 2 [Pa]
E_a	= modulus of elasticity, adhesive [Pa]
F	= force [N]
G_f	= fracture energy [Nm/m^2]
$G_{f\mathrm{I}}$	= fracture energy, mode I [Nm/m^2]
$G_{f\mathrm{II}}$	= fracture energy, mode II [Nm/m^2]
G_s	= modulus of shear, adhesive [Pa]
g	= shape function [—]
ℓ	= length [m]
ℓ_0	= length [m]
P	= force [N]
$P_{\max}$	= maximum tensile load [N]
s	= thickness of adhesive layer [m]
t	= thickness [m]
t_1	= thickness, adherent no. 1 [m]
t_2	= thickness, adherent no. 2 [m]
U_e	= elastic energy [Nm]
W	= crack energy [Nm]
x	= coordinate [m]

α = ratio between adherents [—]
δ = deflection, slip [m]
δ_0 = deflection [m]
δ_1 = deflection [m]
δ_2 = deflection [m]
γ = shear angle [rad]
τ = shear stress [Pa]
τ_1 = shear stress [Pa]
τ_{xy} = local shear stress [Pa]
ω = constant [1/m]
ω_1 = brittleness ratio for lap joints [1/m]

1. Background

At Luleå University of Technology, Sweden, research has been carried out in the area of plate bonding, i.e. the problems that arise when concrete members need to be strengthened using epoxy bonded plates. The research was started in 1988 and is still continuing. Both comprehensive experimental work and theoretical work have been carried out. The laboratory tests include strengthening for bending as well as for shear. A full scale test on a strengthened bridge has also been performed. In the area of theory, the shear and peeling stresses in the adhesive layer at the end of the strengthening plate have been studied in particular, but the theory of fracture mechanics introducing nonlinear behaviour in the joint has also been investigated.

There is great potential for, and considerable economic advantages in, the method of strengthening existing concrete members with epoxy bonded steel or composite plates. If the technique is to be used in an effective manner, it requires a sound understanding of both the short-term and long-term behaviour of the adhesive used. It also requires reliable information concerning the adhesion to concrete and steel or composites. The execution of the bonding work is also of great importance in order to achieve a composite action between the adherents. The utmost importance of knowing within what limits the strengthening method can be used also needs to be mentioned. Although the method of strengthening a structure with plates bonded to it has been used since the mid 1970's, not much attention has been paid to the theory behind the strengthening method. However, since the mid 1980's different theories have been studied and methods to calculate forces and stresses in the adhesive layer have been presented, see Theillout [1], Yuceoglu and Updike [2], Roberts [3–6], Vilnay [7]. Some theories regarding linear fracture mechanics conditions have also been presented, e.g. Hamoush [8], and Hamoush et al. [9, 10].

2. Introduction

The expressions derived in this paper are related to bars strengthened with bonded plates and tested in pure shear, i.e. mode II failure. In the study, both symmetric and non-symmetric overlap joints are considered and analysed with LEFM (Linear Fracture Mechanics) based on energy criteria. Thereafter a one-dimensional NLFM (Nonlinear Fracture Mechanics) analysis is presented for non-symmetric joints.

It is common to denote the fracture energy G_f by $G_{f\text{II}}$ in mode II, but when the mode of fracture is evident from the context the notation G_f is used for the actual mode. However, before starting the derivations we must make the following assumptions:

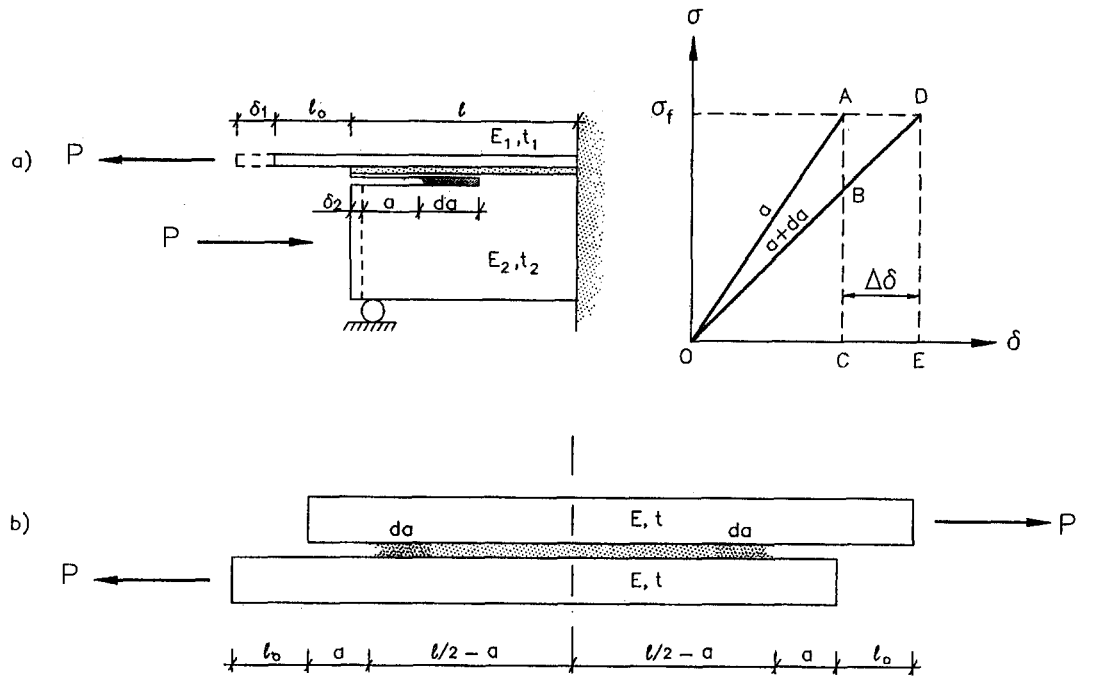

Figure 1. Concrete prisms with bonded plates. The figure also shows a stress-displacement diagram during action of a load P. (a) Non-symmetric case with different materials and stiffness in the adherents; (b) Symmetric case with the same material and stiffness in the adherents.

- the materials are homogenous, isotropic and linear elastic;
- the adhesive is only exposed to shear forces;
- the thickness of the adherents and the adhesive are constant throughout the bond line;
- the width of the steel plate is constant throughout the bond line.

First consider a non-symmetric overlap joint as shown in Figure 1. The energy required for crack growth must be delivered as release of energy. If the adherents are free to move during crack propagation, work is done by the external load. In this case the elastic energy content will increase. For an overlap joint with unit width b, the condition for crack growth can be written as:

$$\frac{\mathrm{d}}{\mathrm{d}a}(U_e - F + W) \leqslant 0 \quad \text{or} \quad \frac{\mathrm{d}}{\mathrm{d}a}\left(F - U_e \geqslant \frac{\mathrm{d}W}{\mathrm{d}a}\right), \tag{1}$$

where U_e is the elastic energy stored in the structure, F is the work done by the external load and W is the energy for crack propagation. Furthermore $G = \mathrm{d}(F - U_e)/\mathrm{d}a$ is *the energy release rate* and $\mathrm{d}W/\mathrm{d}a$ is the *crack resistance force.*

Consider the cracked overlap structure (a) in Figure 1. During the action of the load P, the load application point undergoes a relative displacement $\delta = \delta_1 + \delta_2$. When the crack increases in size by an amount $\mathrm{d}a$ the displacement will increase by an amount $\mathrm{d}\delta$. Thus, the work done by the external force is $P\mathrm{d}\delta$ and (1) can then be rewritten as:

$$G = \frac{\mathrm{d}}{\mathrm{d}a}(F - U_e) = \frac{1}{b}\left(P\frac{\mathrm{d}\delta}{\mathrm{d}a} - \frac{\mathrm{d}U_e}{\mathrm{d}a}\right). \tag{2}$$

The deformations are elastic and, as long as there is no crack growth, the displacement δ is proportional to the load $\delta = PC$, where C is the compliance (inverse of stiffness) of the structure. The elastic energy stored in the structure is:

$$U_e = \tfrac{1}{2}P\delta = \tfrac{1}{2}P^2C. \tag{3}$$

Hence, by using (2) and the chain rule it is then possible to write:

$$G = \frac{1}{b}\left(P^2\frac{\partial C}{\partial a} + PC\frac{\mathrm{d}P}{\mathrm{d}a} - \tfrac{1}{2}P^2\frac{\partial C}{\partial a} - PC\frac{\mathrm{d}P}{\mathrm{d}a}\right) = \frac{P^2}{2b}\frac{\partial C}{\partial a}, \tag{4}$$

or

$$P = \sqrt{2bG\Big/\frac{\partial C}{\partial a}}. \tag{5}$$

It can be shown that (5) also is valid for symmetric overlap joints, see e.g. Wernersson, [11]. It would now be interesting to derive the maximum possible tensile load for a simple symmetric case and for a more complex nonsymmetric case as shown in Figure 1. This will be done next.

2.1. Linear approach

If the deformations in the bars can be considered to be small, and if the influence of moments are neglected and the deformation in the bond layer is not taken into account, then the following change in compliance can be described with the help *of simple beam theory*:

$$\text{Symmetric} \quad \left.\begin{array}{l} C = \frac{\ell_0+a}{EA} + \frac{(\ell/2)-a}{2EA} \\ \frac{\partial C}{\partial da}\frac{1}{2EA} \end{array}\right\}, \tag{6}$$

$$\text{Nonsymmetric} \quad \left.\begin{array}{l} C = \frac{\ell_0+a}{E_1A_1} + \frac{a}{E_2A_2} \\ \frac{\partial C}{\partial a} = \frac{1}{E_1A_1} + \frac{1}{E_2A_2} \end{array}\right\}. \tag{7}$$

With $A_1 = t_1b, A_2 = t_2b$ and $A = tb$, (5), (6) and (7) give us the following expressions for the maximum tensile load:

$$\text{Symmetric} \quad P_{\max} = 2b\sqrt{EtG_f}. \tag{8}$$

$$\text{Nonsymmetric} \quad P_{\max} = b\sqrt{\frac{2E_1t_1G_f}{1+\alpha}}, \tag{9}$$

where

$$\alpha = \frac{E_1t_1}{E_2t_2}.$$

If we compare these equations using the same adherents, i.e. $\alpha = 1$, we see that the equations differ by a factor of 2. This depends partly on the change in compliance and partly on the equilibrium equation for the symmetric case. The derived LEFM equations above give a rough

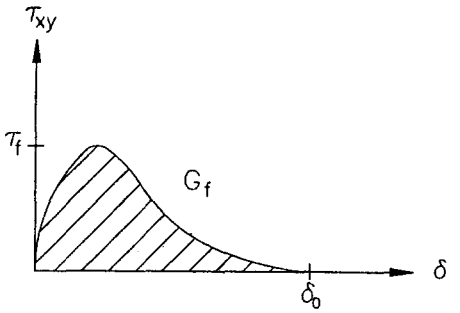

Figure 2. Shear-displacement curve of an adhesive joint according to NLFM.

estimation of the maximum load at failure. If we want a more precise value of the load, more accurate methods are necessary. Hence, it is possible to use NLFM. In this application it is even possible to use a *one-dimensional nonlinear fracture mechanics approach.*

2.2. NONLINEAR APPROACH

Before we start this analysis we must make the assumptions that the bond line is a pure shear medium, i.e. deformation in the bond layer is considered, and the adherents are linear elastic bars in pure tension/compression with no bending effects. The mechanical properties of a bond line are composed of the relation between the local stress τ_{xy} and the local shear displacement δ across the bond line, see Figure 2. If these assumptions are to be valid in mode II fracture it is necessary to introduce *a crack model for shear*, the physical meaning for this model being shown in Figure 3.

Furthermore, the shear strength of the bond zone is denoted τ_f. Another important parameter in NLFM is the fracture energy G_f which is defined as the energy required to bring an area of a bonded surface to complete fracture. This corresponds to the area below the $\tau - \delta$ curve:

$$G_f = \int_0^{\delta_0} \tau \, \mathrm{d}\delta. \tag{10}$$

Since the compatibility and equilibrium equations are the same for nonsymmetric and symmetric joints respectively, the NLFM approach can be applied to both. In Figure 4, a graphic representation of the two types, together with the shear distribution is shown. However, only the nonsymmetric case is presented in the present paper. The derivations in this paper have been made from here following a discussion with Gustafsson, [12].

Study Figure 3 once more. We want to find the critical force $P_{\max}$, corresponding to fracture growth in the bond zone, i.e. when $G = G_f$, where G is the energy release rate and G_f the fracture energy for the joint. The original length of the bond zone is, ℓ. We have a crack length of a and the adherents are homogenous, isotropic and linear elastic where the bond zone is only exposed to shear forces. This means that the bond zone has an actual length of $\ell - a$. The derived expression for the shear stress can therefore be written as:

$$\tau(x) = \frac{P_{\max}\omega}{b} \frac{\cosh(\omega x)}{\sinh(\omega(\ell - a))}, \quad 0 \leqslant x \leqslant \ell - a \tag{11}$$

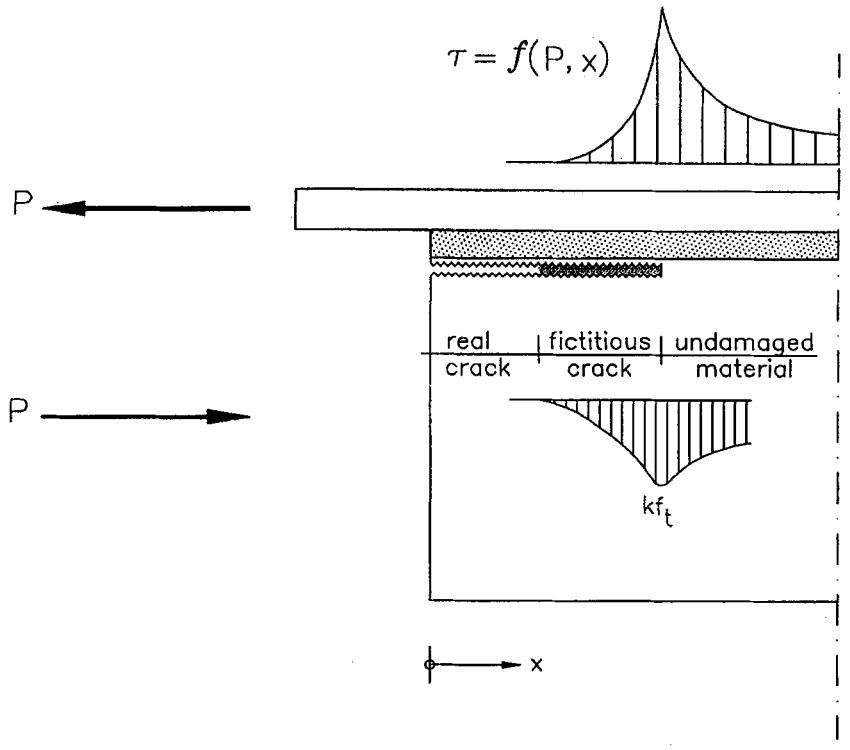

Figure 3. Crack model for shear.

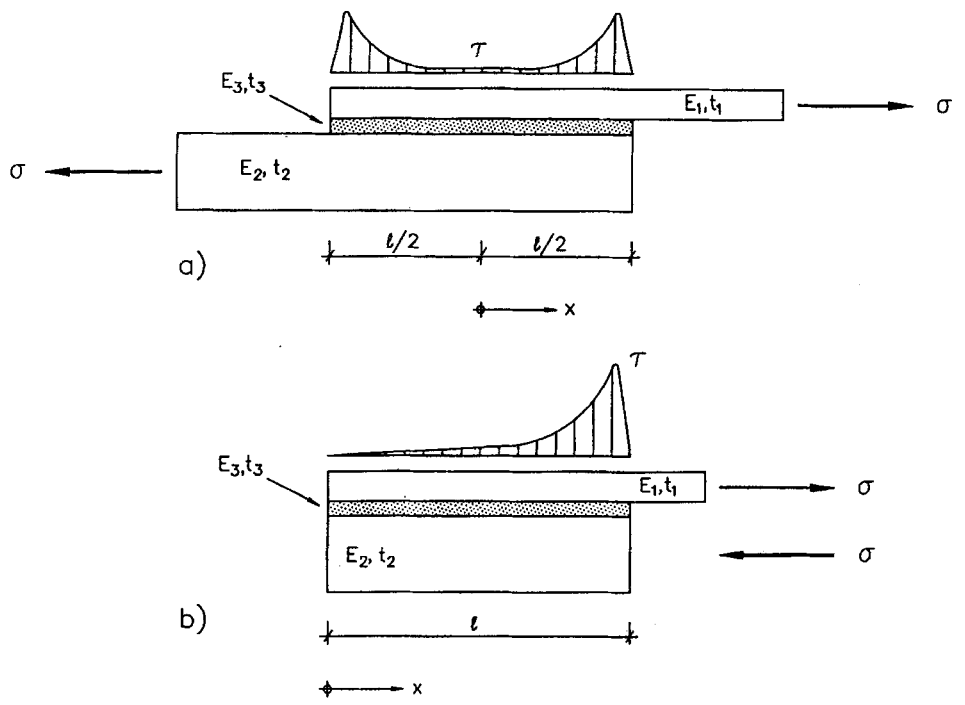

Figure 4. Shear distribution for symmetric and non-symmetric overlap joints.

and

$$\omega^2 = \frac{G_s}{s}\left(\frac{1}{E_1 t_1} + \frac{1}{E_2 t_2}\right), \tag{12}$$

where s is the thickness of the adhesive G_s, the shear modulus in the adhesive, and $E_1 t_1$ and $E_2 t_2$ are the stiffness for the adherents respectively, see also Täljsten, [13].

Study Figure 5 (a) and (b). We have two situations. One when the size of the crack is a, and one when the length of the crack has increased from a to $a + \mathrm{d}a$. To move from (b) to (a), a certain amount of work is needed (to bring the crack together). This work can be expressed as:

$$W_e = \int_{\ell-(a+da)}^{\ell-a} \left[\int_0^{\gamma(x)} \underbrace{b\tau(\gamma)}_{\text{force/unitlength}} \underbrace{sd\gamma}_{\text{distance}} \right] \mathrm{d}x. \tag{13}$$

As the opposite of the work needed to bring the crack together, the *energy release rate* G when we move from (a) to (b), over the crack surface bda, can consequently be written:

$$G = \frac{1}{bda} \int_{\ell-(a+da)}^{\ell-a} \left[\int_0^{\gamma(x)} b\tau(\gamma) s d\gamma \right] \mathrm{d}x \tag{14}$$

and if we enter the limits for the integrals in (14) we obtain:

$$\begin{aligned} G &= \frac{1}{bda}[(\ell - a) - (\ell - (a + da))] \int_0^{\gamma(x)} b\tau(\gamma) s d\gamma, \\ &= s \int_0^{\gamma(s)} \tau(\gamma) d\gamma \quad \text{in general.} \end{aligned} \tag{15}$$

However, $\tau(\gamma) = \tau = G_s\gamma$ in the case when the bond zone is linear elastic. Equation (15) can then be written:

$$G = \frac{sG_s\gamma_1^2}{2} = \frac{s\tau_1^2}{2G_s}, \tag{16}$$

where τ_1 is the shear stress at the end of the bond zone, i.e. at the loaded end of the specimen in the case studied.

When $x = \ell - a$ (11) together with (16) can be expressed as:

$$G = \frac{s}{2G_s} \frac{\omega^2 P^2}{b^2} \frac{1}{\tanh^2(\omega(\ell - a))}. \tag{17}$$

When $G = G_f$ then $P = P_{\max}$, i.e.:

$$G_f = \frac{s}{2G_s} \frac{\omega^2 P_{\max}^2}{b^2} \frac{1}{\tanh^2(\omega(\ell - a))}, \tag{18}$$

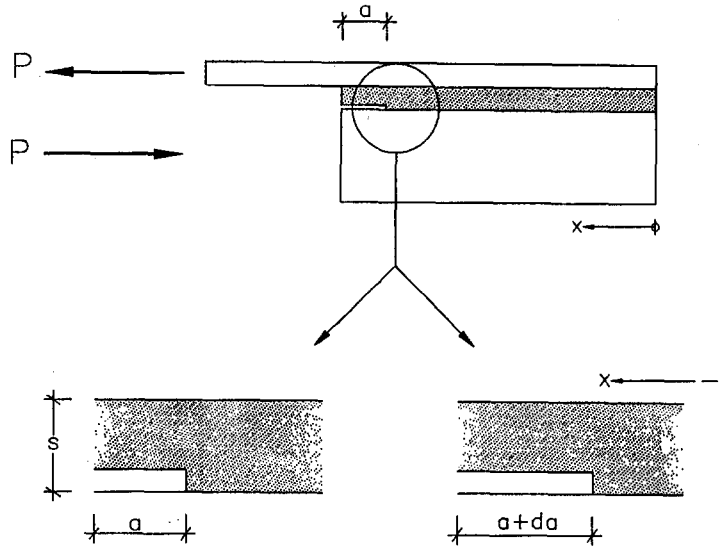

Figure 5. Crack growth in the studied bond zone.

or

$$P_{\max} = \sqrt{\frac{2G_s G}{s}} \frac{b}{\omega} \tanh(\omega(\ell - a)) \tag{19}$$

and

$$G_f = \frac{s\tau_1^2}{2G_s}. \tag{20}$$

Figure 6 (a) gives, when $x = \ell - a$, that $\tau_1 = \tau_f$ and (20) can be written as:

$$G_f = \frac{s\tau_f^2}{sG_s}. \tag{21}$$

Consequently (19) can be written as:

$$P_{\max} = \frac{b\tau_f}{\omega} \tanh(\omega(\ell - a)). \tag{22}$$

Equation (22) can be normalised if we divide the expression by $\tau_f b(\ell - a)$:

$$\frac{P_{\max}}{\tau_f b(\ell - a)} = \frac{\tanh(\omega(\ell - a))}{\omega(\ell - a)}. \tag{23}$$

Equation (23) can be simplified if we introduce a new notation ω_1 (different from ω in (12)).

$$\omega_1^2 = 2\omega^2(\ell - a) = \frac{\tau_f^2(\ell - a)^2(1 + \alpha)}{E_1 t_1 G_f}, \tag{24}$$

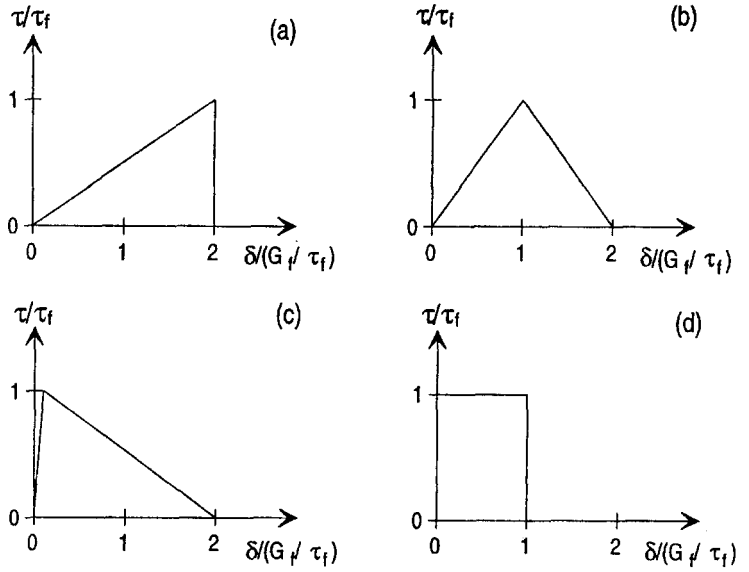

Figure 6. Different simplified shapes of $\tau - \delta$ curves, from Gustafsson, [14].

where the normalised load-carrying capacity is governed by the ratio $\omega_1^2 = \tau_f^2(\ell - a)^2(1 + \alpha)/E_1 t_1 G_f$, which is commonly referred to *as the brittleness ratio for lap joints*, see e.g. Gustafsson, [14] and Wernersson, [11, 15]. High values of the brittleness ratio correspond to fracture by crack propagation and low values to a fairly uniform stress throughout the bond line during fracture. Hence, it is clear that the maximum normalised load in general can be written as:

$$\frac{P_{\max}}{\tau_f b(\ell - a)} = F\left(\frac{\tau_f^2(\ell - a)^2}{E_1 t_1 G_f}, \alpha, g\right), \tag{25}$$

where g represents the shape function of the $\tau - \delta$ curve. Different simplified shapes of $\tau - \delta$ curves have been presented in [14], see Figure 6. From these simplified curves it is possible to solve (25) analytically. For a more realistic shape of the $\tau - \delta$ curve, numerical stepwise calculations are needed. For curve (a) in Figure 6, (25) can be expressed in the following way:

$$\frac{P_{\max}}{\tau_f b(\ell - a)} = \frac{\sqrt{2}}{\omega_1}\tanh\left(\frac{\omega_1}{\sqrt{2}}\right). \tag{26}$$

It is now possible to establish two extreme cases for a joint. In the first case we have a ductile adhesive with a low value of ω_f, and in the second case we have a more brittle adhesive with a quite high value of ω_1. In the first case τ_f is the governing bond zone parameter and in the second case G_f is the governing bond zone parameter. The latter is the case for most of the epoxy adhesives used. Equation (26) can then be written as:

Ductile $P_{\max} \approx \tau_f b(\ell - a)$ when $\omega_1 < 0.1$,

In general $\dfrac{P_{\max}}{\tau_f b(\ell - a)} = \dfrac{\sqrt{2}}{\omega_1}\tanh\left(\dfrac{\omega_1}{\sqrt{2}}\right)$ all ω_1,

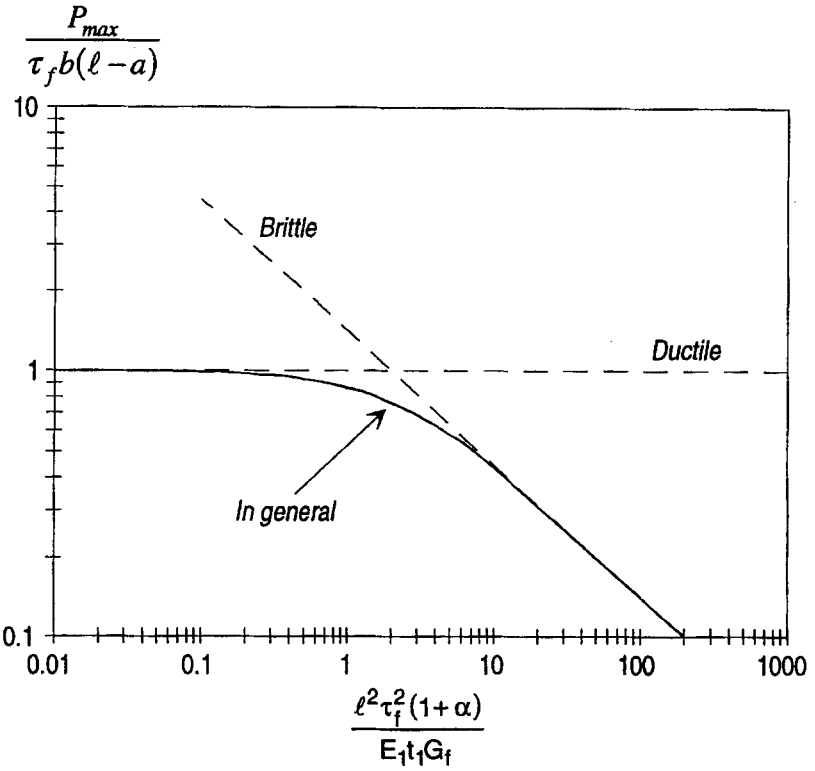

Figure 7. Normalised joint strength as a function of the brittleness ratio for symmetric and non-symmetric lap joints. Similar curves for symmetric lap joints have been presented in [14].

$$\text{Brittle} \quad P_{\max} \approx b\sqrt{\frac{2E_1 t_1 G_f}{1+\alpha}} \quad \text{when} \quad \omega_1 > 3.0.$$

The cases are illustrated in Figure 7. The curve marked 'In general' is plotted here for (26). A similar figure for symmetric joints was presented in [14], [16] and [17].

3. Comparison with theory and tests

To gain an understanding of what happens during the propagation of a crack in the adherent along the bond line parallel with a steel or a FRP (Fibre Reinforced Plastic) plate, tests in shear have been made. One of the aims of these tests was to determine the anchor lengths which give a more effective force transfer between the adherents. This is not recorded here, instead you are referred to [13]. However, the main objective is to explain what happens during the propagation of a crack in the concrete.

The test equipment used is shown in Figure 8, where a schematic sketch is presented. In the sketch a concrete prism on two supports is placed on a steel beam. The tensile force is applied by a hydraulic jack and transferred through a moment-free link to the strengthening plate. The hydraulic jack can also be moved in the vertical direction to minimise the negative effect of any moment introduced by the angle between the strengthening plate and the load level arm. All of the tests were position-controlled by an LVDT gauge. The load rate varied between 0.0002 mm/s and 0.0020 mm/s, but were kept constant during each type of test.

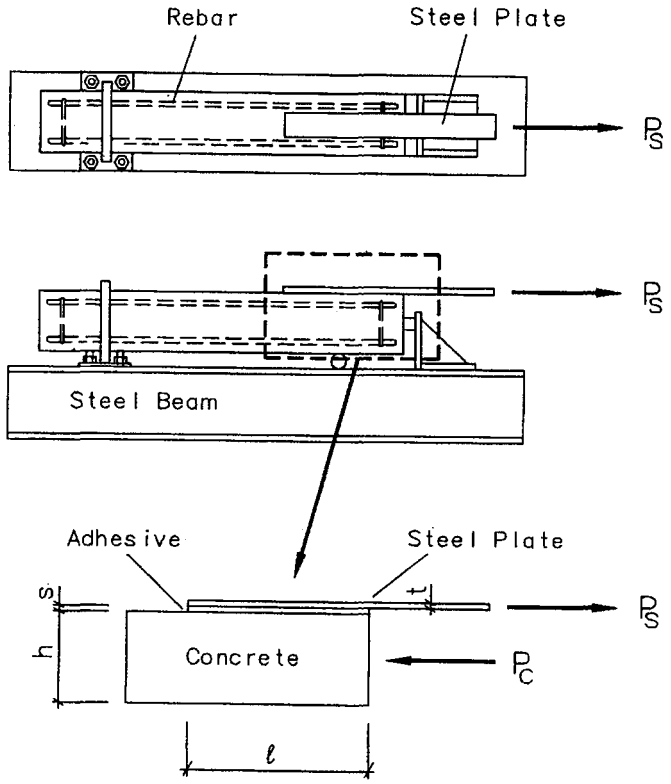

Figure 8. Schematic sketch of the test equipment used in the tensile test series.

The results from the tests can be compared with the fracture mechanics model derived earlier, i.e. (26).

$$\frac{P_{\max}}{\tau_f b((\ell - a))} = \frac{\sqrt{2}}{\omega_1}\tanh\left(\frac{\omega_1}{\sqrt{2}}\right).$$

In the case of a quite stiff bond zone, a good approximation can be written:

$$P \approx b\sqrt{\frac{2E_s t G_f}{1+\alpha}}, \tag{27}$$

or

$$\varepsilon \approx \sqrt{\frac{2G_f}{E_s t(1+\alpha)}}, \tag{28}$$

where ε is the measured strain at the top strengthening plate. In (27) and (28) we can notice that the fracture energy for the concrete is needed (since the failure always happens in the concrete). However, it is very difficult to measure the pure mode II fracture energy and extensive test equipment is required, see e.g. Hassanzadeh, [18]. Since we were not able to measure the pure mode II fracture energy, tests were performed in mode I and only approximation tests to try to find the mode II fracture energy were performed, see [13]. However, the measured

Table 1.

Test No.	E [MPa]	t [mm]	α	P_{max} [kN]	ε_{max} [μs]	P_I [μ s]	P_{II}	ε_I	ε_{II}
S400 40A	205	2.9	0.123	41.1	1728	15.2	45.1	641	1905
S400 60A	205	2.9	0.123	58.4	1637	22.9	68.0	641	1905
S400 60B	205	2.9	0.123	53.0	1486	22.9	68.0	641	1905
S500 80C	205	2.9	0.123	67.3	1415	30.5	90.6	641	1905
S600 80B	205	2.9	0.123	71.4	1501	30.5	90.6	641	1905
S800 80A	205	2.9	0.123	61.6	1295	30.5	90.6	641	1905
G200 80A	23	0.9	0	21.9	13225	6.0	17.8	3640	10817
G500 80A	23	0.9	0	24.1	14553	6.0	17.8	3640	10817
C300 50A	162	1.2	0.04	35.1	3611	11.3	33.6	1164	3459
C400 50A	162	1.2	0.04	26.9	2768	11.3	33.6	1164	3459

fracture energies in mode I underestimates the load-carrying capacity at fracture whereas the approximation mode II fracture energies overestimates it. Nevertheless, the measured fracture energies give the limits within which the load-carrying capacity should be contained.

In Table 1 comparison is made between test results from pure shear tests and (27) and (28). Notice also that (27) and (28) do not consider the length of the anchor zone; therefore the comparison is made for those tests having anchor lengths exceeding the critical one, i.e. 300 mm, see [13]. In the calculations, the mean value from the fracture energies has been used, i.e. $\bar{G}_{fI} = 137.1 \pm 14.9\,\text{nm/m}^2$ and $\bar{G}_{fII} = 1210.7 \pm 462.1\,\text{nm/m}^2$, and α is calculated for each series in accordance with (9) with $E_c = 25.0\,\text{GPa}$. In Table 1, P_{max} and ε_{max} denote measured force and calculated strain in the steel plate related to this force. Furthermore, Tests No. S400 40A shows tests with mild steel plates, length 400 mm and width 40 mm, test A, G denotes glass fibre reinforced plastic and C plates of carbon fibre reinforced plastic.

No firm conclusions can be drawn from the comparison of the performed tests in Table 1. This is mainly due to the fact that it is very difficult to measure pure mode fracture in concrete. However, what can be seen in Table 1 is that the measured values for all the test specimens studied, except for test series G, lie between the values calculated from the measured fracture energies. A preceding source of error that needs to be mentioned is the use of the simplified load-deflection curve, curve (a) in Figure 6. Thus this error cannot be very large since tests of the adhesive used correspond quite well with the assumed curve. However, when using different types of adhesives or very weak adherent materials, the bond zone curve for the case studied should be used and numerical calculations are needed.

4. Conclusions

Pure shear tests on concrete prisms strengthened with mild steel, CFRP and GFRP plates have been performed. In connection with these tests linear and nonlinear fracture mechanics equations have been derived.

It is quite easy to study these test specimens in the elastic domain by use of linear fracture mechanics (LEFM) methods; however, when the concrete starts to fracture, nonlinear methods have to be used.

In this paper, a new nonlinear fracture mechanics (NLFM) approach has been derived, introducing a new model called the fictitious crack model for shear. This model is based on the fracture mechanics criterion from Hillerborg, [19], and Gustafsson, [14]. The fundamental idea with the NLFM theory is that all the elastic energy created by the shear stress over a unit length will be used to create a new crack in the bond zone. The elastic energy is calculated, and by using a known or assumed shear slip curve, the nonlinear behaviour of the studied joint can be predicted. Since quite stiff adhesives have been used in this study, the shear-slip curve is almost linear and the complicated equations derived can be simplified for calculation purposes. The fracture is a shear failure (mode II). The shear (mode II) fracture energy is difficult to measure and therefore, only rough tests could be made and compared to theoretical values. Nevertheless, the test results indicate that this method can be used to calculate fracture in concrete joints loaded in pure shear. However, for weak bond zones, the calculation can be complicated and numerical methods are needed.

Acknowledgement

Financial support has been provided by the Swedish Council for Building Research, the Swedish National Road Administration and Nils Malmgren AB. Furthermore, the assistance of Professor Lennart Elfgren has been greatly appreciated.

References

1. J.N. Theillout, Renforcements de structures par la technique des tôles collées. In *Proceedings of IABSE Symposium of Durability of Structures*, Lisbon, September 1989, 767–772.
2. U. Yuceoglu and D.P. Updike, Stress analysis of bonded plates and joints. *Journal of the Engineering Mechanics Division* (1980) 37–56.
3. T.M. Roberts, Finite difference analysis of composite beams with partial interaction. *International Journal of Computers & Structures* 21:3 (1984) 469–473.
4. T.M. Roberts, Approximate analysis of shear and normal stress concentrations in the adhesive layer of plated RC-beams. *The Structural Engineer* 67:12 (1989) 229–233.
5. T.M. Roberts, Shear and normal stresses in adhesive joints. *Journal of Engineering Mechanics* 115:11 (1989) 2460–2476.
6. T.M. Roberts, Analysis of stress concentrations in the adhesive layer of plated concrete beams. International Seminar on Structural Repairs/Strengthening by the Plate Bonding Technique, University of Sheffield (1990) 11.
7. O. Vilney, The analysis of reinforced concrete beams strengthened by epoxy bonded steel plates. *International Journal of Cement Composites and Ligthweight Concrete* 10:2 (1988) 73–78.
8. S.A. Hamoush, A Fracturing Model for Concrete Beams Strengthened by Externally Bonded Steel Plates, PhD. thesis, North Carolina State University (1988) 226.
9. S.A. Hamoush and S.H. Ahmad, Debonding of steel plate-strengthened concrete beams. *Journal of Structural Engineering* 116:2 (1990) 356–371.
10. S.A. Hamoush and S.H. Ahmad, Static strength of steel plate strengthened concrete beams. *Materials and Structures/Matèriaux et Constructions* 23 (1990) 116–125.
11. H. Wernersson, Wood Adhesive Bonds, Fracture Softening Properties in Shear and in Tension, Report TVSM-3012, Lund Institute of Technology (1994) 156.
12. P.J. Gustafsson, Private discussion, Lund Institute of Technology (1994).
13. B. Täljsten, Plate Bonding, Strengthening of Existing Concrete Structures with Epoxy Bonded Plates of Steel or Fibre Reinforced Plastics, Doctoral thesis, Luleå University of Technology (1994) 308.
14. P.J. Gustafsson, Analysis of generalized Volkersen-Joints in terms of nonlinear fracture mechanics. In *Mechanical Behaviour of Adhesive Joints*, Edition Pluralis, G. Verchery and A.H. Cardon (eds), Paris (1987) 139–150.
15. H. Wernersson, Fracture Characterization of Wood Adhesive Joints, PhD. thesis, Lund Institute of Technology (1994) 156.
16. P.J. Gustafsson and H. Wernersson, in *Analysis of Concrete Structures by Fracture Mechanics*, a RILEN report, L. Elfgren and S.P. Shah (eds.) Chapman & Hall, Sweden (1989) 220–233.

17. P.J. Gustafsson and H. Ernersson, Modelling, Testing and Strength Analysis of Adhesive Bonds in Pure Shear, Report TVSM 7039, Lund Institute of Technology (1987) 29.
18. M. Hassanzadeh, Behaviour of Fracture Process Zones in Concrete Influenced by Simultaneously Applied Normal and Shear Displacements, PhD. thesis, Lund Institute of Technology (1992) 104.
19. A. Hillerborg, Materialbrott (Material Failure), Report TVBM-3004, Lund Institute of Technology (1977) 48.